Swiss J Geosci (2012) 105:19–38
DOI 10.1007/s00015-011-0089-6

Syn-thrust deformation across a transverse zone: the Grem–Vedra fault system (central Southern Alps, N Italy)

Andrea Zanchi · Paolo D'Adda · Stefano Zanchetta · Fabrizio Berra

Received: 21 October 2010 / Accepted: 25 October 2011 / Published online: 10 January 2012

Abstract The lateral continuity of the E–W trending thrust sheets developed within the Lower to Middle Triassic cover of the central Southern Alps (Orobic belt) is disturbed by the occurrence of several N–S trending transverse zones, such as the poorly known Grem–Vedra Transverse Zone (GVTZ). The GVTZ developed during the emplacement of the up to six S-verging thrust sheets consisting of Lower to Middle Triassic units, occurring immediately south of the Orobic Anticlines. The transverse zone, active during thrust emplacement related to the early Alpine compressions which pre-date the Adamello intrusion, includes three major vertical shear zones, the Grem, Pezzel and Zuccone faults. The major structure of the transverse zone is the dextral Grem fault, forming a deep lateral ramp between thrust sheets 3 and 5. A similar evolution also occurred along the Zuccone and Pezzel faults, which show a left-lateral displacement of syn-thrust folds. The Grem fault was later reactivated as an oblique tear fault during the emplacement of the Orobic Anticlines, due to back-thrusting along out-of-sequence thrust surfaces (Clusone fault). Transpressional deformations along the fault zone are recorded by the rotation of major syn-thrust folds, which also suggest a horizontal offset close to 0.5 km. Records of the first stage of evolution of the Grem fault are better preserved along its northern segment, and structural relationships suggest that it propagated southward and downward in the growing thrust stack. The study of the meso and megascopic structures developed along the GVTZ constrains the evolution of the transverse zone, illustrating the complex deformational phenomena occurring in a transpressional regime. The GVTZ probably reflects the existence of pre-existing tectonic lineaments with a similar orientation. Evidence of pre-existing structures are not preserved in the exposed units, nevertheless the N–S extensional fault systems that characterize the Norian to Jurassic rifting history of the Lombardian basin are valid candidates.

Keywords Alpine tectonics · Southern Alps · Fold-and-thrust belt · Tectonic evolution · Fault reactivation · Transpressional regime

1 Introduction

Transverse zones affect fold-and-thrust belts and play a major role during their evolution, as they represent regional across-strike shear zones displacing adjacent sectors characterized by different deformation styles and/or amounts of shortening. These complex and articulated structures are the site for the development of tear faults and lateral ramps that interact with frontal ramps and thrust-related folds, causing abrupt along-strike changes in the lateral continuity of thrust-stacks. The location of transverse zones within an orogenic belt are related to different controlling factors (Thomas 1990). Possible controls can be ascribed to changes in the tectonic regime or the existence of older tectonic lineaments or abrupt lithological changes, which act as weakness zones able to drive the development of these

Editorial handling: A.G. Milnes.

A. Zanchi (✉) · P. D'Adda · S. Zanchetta
Dipartimento di Scienze Geologiche e Geotecnologie, Università degli Studi di Milano-Bicocca, Piazza della Scienza 4, 20126 Milano, Italy
e-mail: andrea.zanchi@unimib.it

F. Berra
Dipartimento di Scienze della Terra "A. Desio", Università degli Studi di Milano, Via Mangiagalli 34, 20133 Milano, Italy

structures. The study of transverse zones is favoured when they are developed within sedimentary units with a well-known stratigraphic setting, since it is then possible to use stratigraphic markers to confidently constrain (a) the throw of the faults and (b) the correlation of tectonic units across the transverse zone. A favourable area for the study of transverse zones is represented by the fold-and-thrust belt of the Italian Southern Alps, which is segmented by the occurrence of important transverse zones (Laubscher 1985; Schönborn 1992a, b). They generally reflect the reactivation of Upper Triassic to Jurassic normal faults related to the Mesozoic evolution of the South Alpine domain (Gaetani and Jadoul 1987; Bernoulli 2007), which are oriented roughly parallel to the Alpine compression (Berra and Carminati 2010 and references therein). The major example of this kind in the Southern Alps is the Giudicarie line, which represents the reactivation of a Mesozoic paleogeographic lineament separating the Trento Plateau from the Lombardian Basin (Castellarin et al. 2006 for a synthesis). In the central Southern Alps, Schönborn (1992a) described other transverse zones, as the Faggio–Morterone, the Lugano and the Lake Lecco lines, whose position is controlled by the reactivation of Jurassic extensional faults which deeply interacted with the emplacement of thrust units during the Alpine compressions.

Another interesting transverse structure is represented by the poorly-known Grem–Vedra Transverse Zone (GVTZ), which is located in the central sector of the Southern Alps (Orobic Alps). Although the fault system was identified and described already at the beginning of systematic studies in the Orobic Alps (De Sitter and De Sitter-Koomans, 1949), due to the presence of Zn-related ore deposits of the Gorno mine district across the GVTZ, its interpretation is still controversial (Schönborn 1992a; Forcella and Jadoul 2000). An important, often ignored, contribution to the understanding of the deep structure of the fault system was given by Rodeghiero and Vailati (1978), describing in detail the geological setting reconstructed during the excavation of deep mining tunnels crossing the Grem fault at depth.

The aim of this paper is to describe this complex N–S transverse zone providing a detailed scheme of its geometrical and structural setting, in order to understand its role during the tectonic evolution of the central Southern Alps. The reconstruction of the GVTZ is supported by the production of a 3D geological model, which was built in order to validate our structural interpretation and obtain intelligible 3D visualizations of the main structures.

The kinematic history of the GVTZ has been also related to the relative chronology of the major deformation events occurring in the Southern Alps, contributing to the reconstruction of the evolution of the entire thrust belt.

2 Regional setting

The South Alpine zone (Fig. 1a, b) developed south of the E–W trending Insubric line (Schmid et al. 1989) and was deformed during the Alpine orogeny under very low- to non-metamorphic conditions. A complex S-verging, thick-skinned fold-and-thrust belt formed over a basal décollement (Fig. 1c) that deepens regularly from 5 km under the Po plain to 16 km near the Insubric line (Gaetani and Jadoul 1979; Pieri and Groppi 1981; Carminati and Siletto 1997; Carminati et al. 1997; Schumacher et al. 1997). Thrust sheets involve the Variscan metamorphic basement in the northern sector of the belt and the Permo-Mesozoic sedimentary cover in its southern part, defining different structural E–W trending sub-domains.

The Orobic Thrust (Fig. 1a) is the northernmost thrust surface, along which the basement is stacked southward onto the Permian to Induan sedimentary cover. It is generally represented as a single thrust fault, associated in its eastern sector with imbricate structures reactivating Permian transtensional faults (Blom and Passchier 1997). South of this line three WSW–ENE trending regional anticlines are present (Orobic Anticlines, Fig. 1b), affecting the metamorphic basement and its Permian cover. To the south, the Orobic Anticlines are bounded by an E–W striking, south-dipping fault (Valtorta–Valcanale fault). South of this fault, an E–W trending antiformal thrust stack occurs. The imbricates exposed in the antiformal stack consist of Lower Triassic to Carnian rocks, forming large S-verging thrust sheets developed along two main décollement horizons: the Olenekian Carniola di Bovegno at the base, and the Carnian San Giovanni Bianco Fm at the top. Southward these units wedge below an Upper Triassic succession along the south-dipping Clusone fault (Fig. 1b, c), which represents the detachment horizon of the Upper Triassic units over the Lower–Middle Triassic ones (Zanchi et al. 1990). The most external part of this belt also includes to the south the Jurassic and Cretaceous successions, unconformably covered by the Oligo–Miocene foredeep deposits of the Gonfolite Lombarda and related sediments, which form the so-called Milano Belt (Laubscher 1985), deeply buried below the post-Tortonian Po basin fill.

The reconstruction of the chronology of the major deformation events affecting the Orobic belt during the Alpine orogeny has been the subject of different regional studies (Laubscher 1985; Zanchi et al. 1990a; Schönborn 1992a; Fantoni et al. 1999; Castellarin et al. 2006; Zanchetta et al. 2011; D'Adda et al. 2011) which document at least two stages of thrusting predating the Late Eocene—Early Oligocene intrusion of the Adamello batholith. The Oligo–Miocene tectonic activity of the belt, involving the coeval foredeep deposits formed along its southern front,

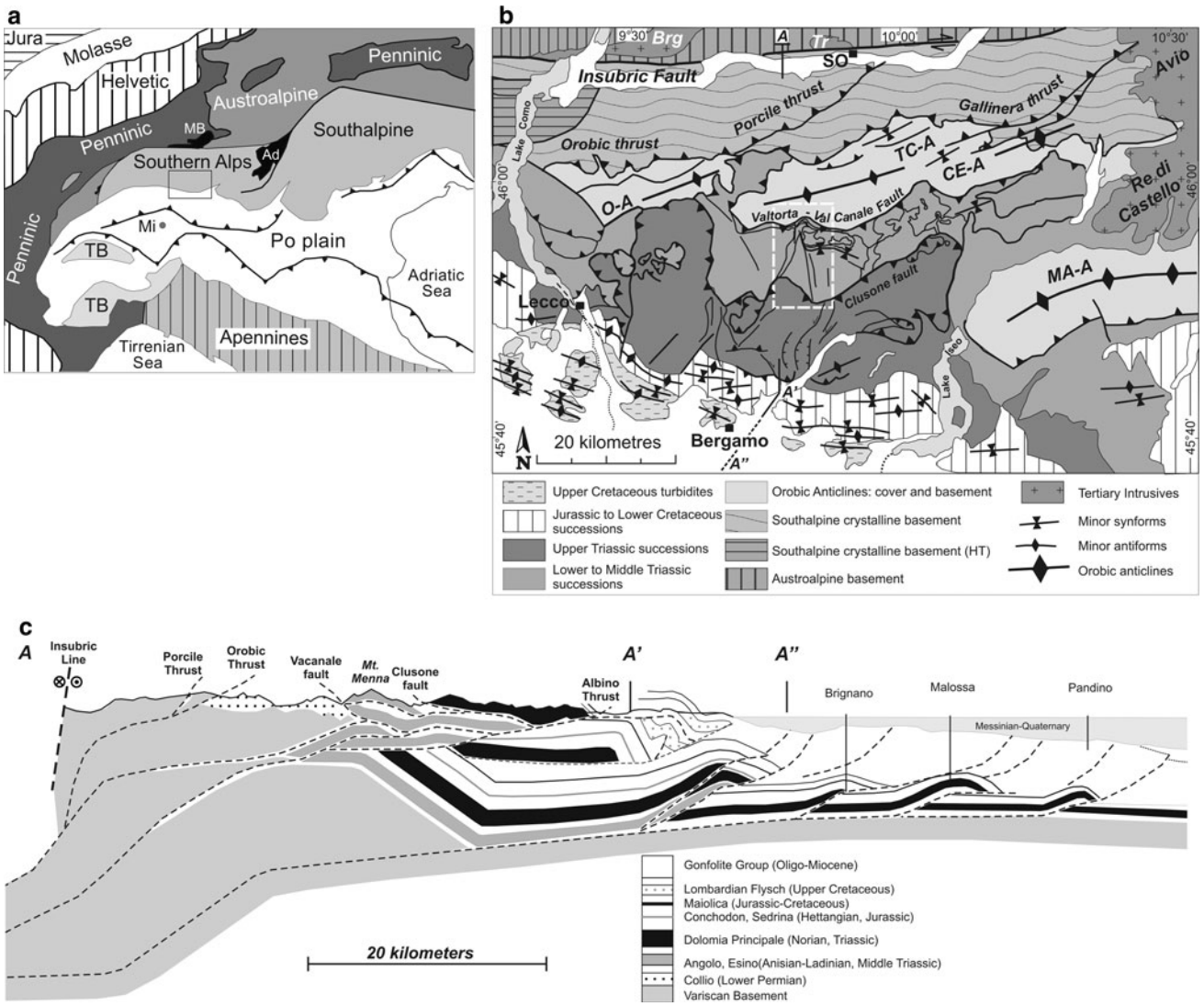

Fig. 1 **a** General structure of the Alps with location of **b**. *MB* Masino–Bregaglia, *Ad* Adamello, *TB* Piedmont Tertiary Basin, *Mi* Milan. **b** Geological sketch of the central (Orobic) Southern Alps, N Italy. *Brg* Masino–Bregaglia, *Tr* Triangia, *SO* Sondrio, *O-A* Orobic Anticline, *TC-A* Trabuchello–Cabianca Anticline, *CE-A*: Cedegolo Anticline, *MA-A* Maniva Anticline. **c** General cross section along the Southern Alps, modified from Schönborn (1992b)

represents a younger well-documented tectonic event (Pieri and Groppi 1981; Gelati et al. 1991; Fantoni et al. 1999; Bersezio et al. 2001; Castellarin et al. 2006).

3 Geological and structural setting of the Grem–Vedra transverse zone (GVTZ)

The location of the study area is shown in Fig. 1b and the geological and structural data are compiled in Figs. 2, 3 and 4. The area includes part of the southern side of the Orobic Anticlines system, the Lower–Middle Triassic imbricates and the northern sector of the Upper Triassic succession. These different structural domains have a general E–W trend and are separated from each other by two main lineaments: the Valtorta–Valcanale fault to the north and the Clusone fault to the south (Figs. 2, 3). North of the Valtorta–Valcanale fault, a Permian-Lower Triassic succession occurs (Trabuchello–Cabianca Anticline), including the Lower Permian volcanic and volcaniclastic successions of the Pizzo del Diavolo Fm. and Cabianca Vulcanite (Collio Formation *Auctorum*), unconformably covered by the Upper Permian red conglomerates and sandstones of the Verrucano Lombardo, up to the Induan–Olenekian quartz-sandstones and siltstones of the Servino.

The Lower Triassic to Carnian succession to the south is arranged in a number of S-verging ramp-and-flat thrust systems which form a thrust stack with a regional antiformal arrangement (Figs. 1c, 4). The oldest unit in the antiformal stack is represented by the sabkha facies of the

Fig. 2 Geological-structural map of the GVTZ from original field mapping at 1:5,000 and 1:10,000 scale. Key to fault nomenclature (applies to all succeeding figures): N Grem fault, northern segment of the Grem fault; S Grem fault, southern segment of the Grem fault; E Grem fault, Eastern Grem fault. Traces of N–S cross sections of Fig. 4 and E–W traces of Figs. 7 and 8 are shown

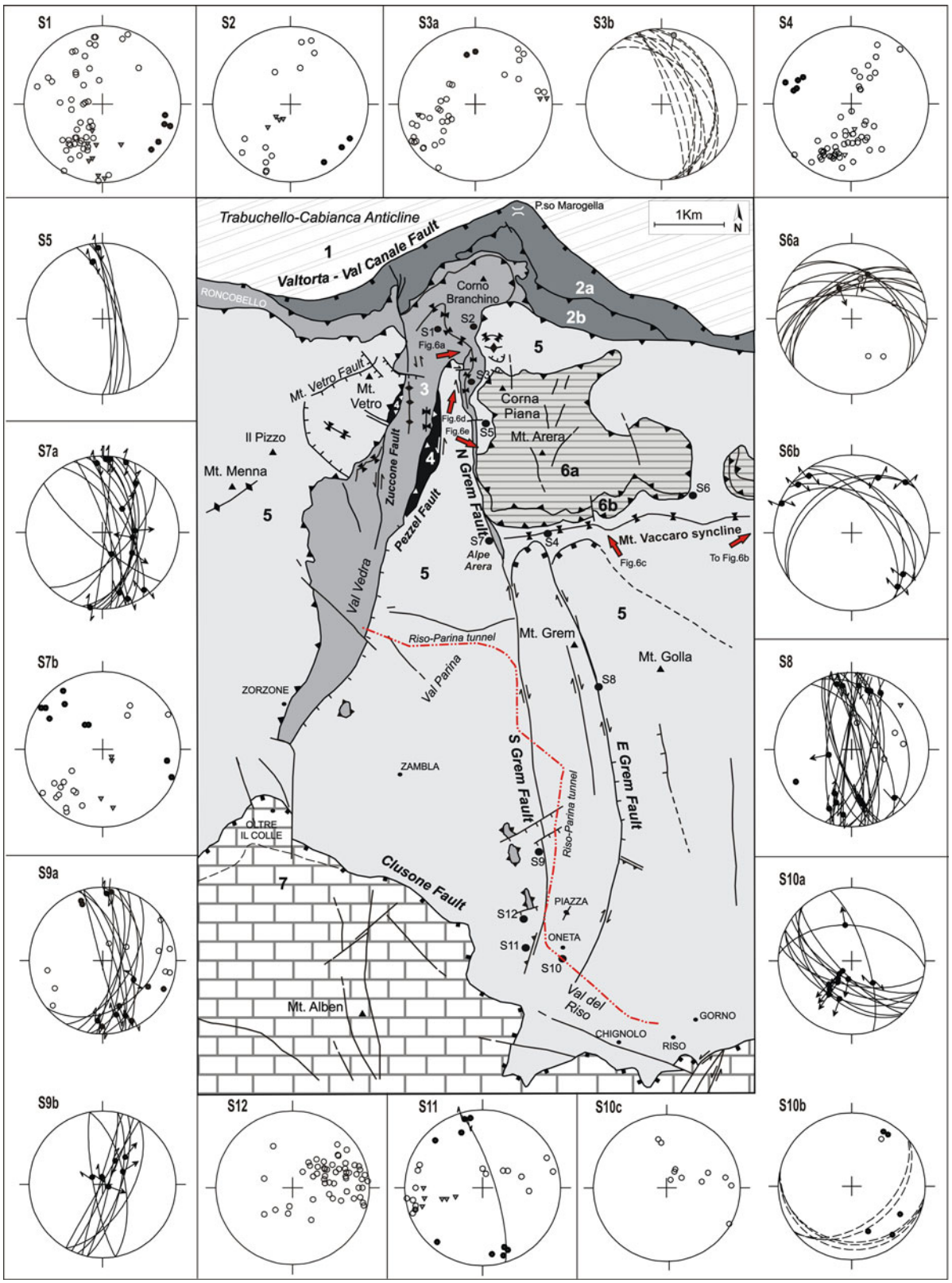

Fig. 3 Interpretative tectonic scheme of the study area. The main tectonic units (see text for description) were identified on the base of mesostructural and stratigraphic analyses. Fault attitude and kinematics are described in the correlated stereographic projections (equal area, lower hemisphere). The trace of the Riso-Parina tunnel cross-cutting the GVTZ at depth is also indicated. The location of the field photos of Fig. 6 is given by *arrows*

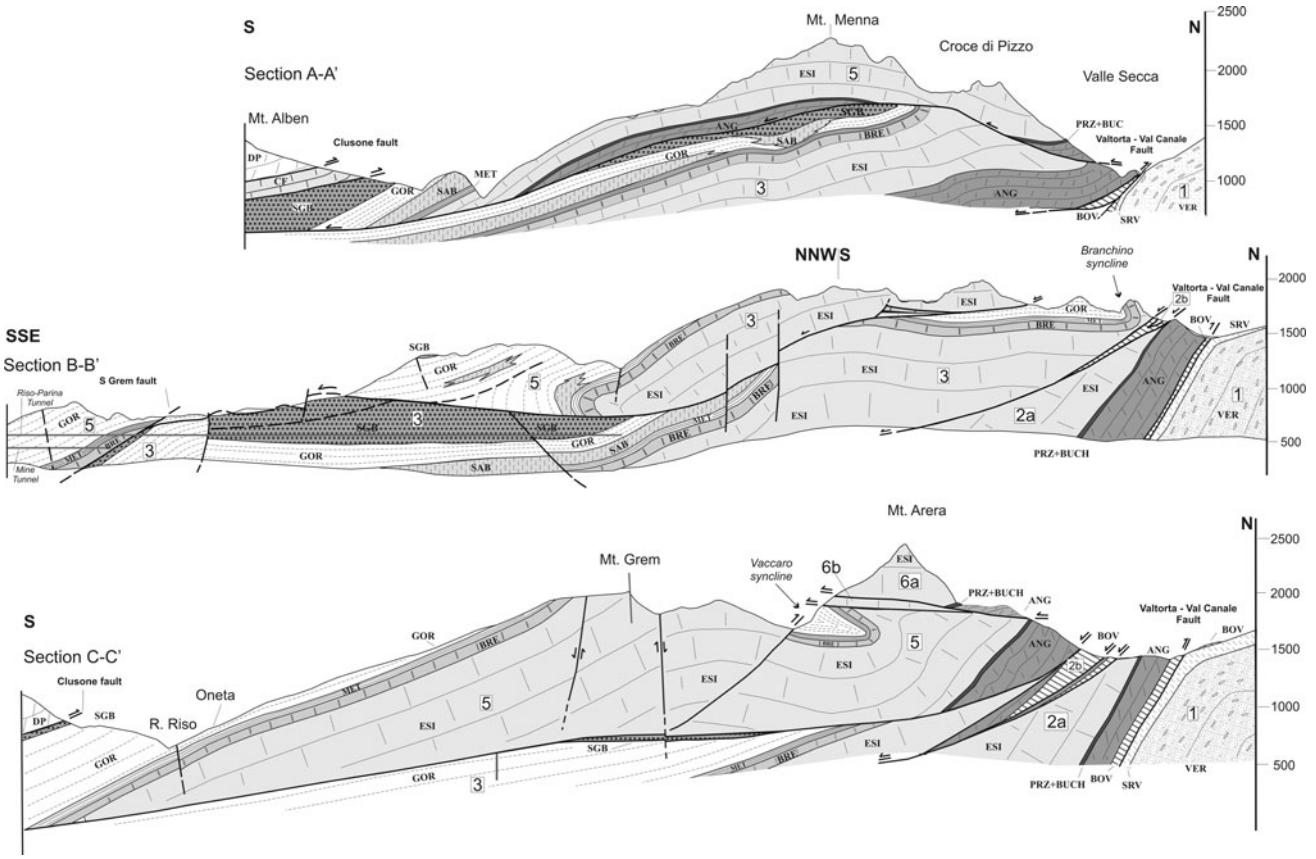

Fig. 4 N–S cross-sections. Cross section A–A' and C–C' are located outside the GVTZ, to the W and E respectively. The B–B' cross-section trace is entirely within the GVTZ. The location of the cross-section traces are shown on the geological map of Fig. 2. Cross sections by Rodeghiero and Vailati (1978) have been considered for the southern part of the area. *VER* Verrucano Lombardo, *SRV* Servino, *BOV* Carniola di Bovegno, *ANG* Angolo Limestone, *PRZ* Prezzo Limestone, *BUCH* Buchenstein Formation, *ESI* Esino Limestone, *BRE* Breno Formation, *MET* Metallifero Bergamasco Limestone, *GOR* Gorno Formation, *SAB* Val Sabbia Sandstone, *SGB* San Giovanni Bianco Formation, *CF* Castro Formation, *DP* Dolomia Principale

Carniola di Bovegno, consisting of evaporitic dolostones with gypsum layers occurring along the main thrust surfaces as tectonic slices. The Anisian to Carnian succession shows a few local variations within the mapped units (Figs. 2, 5); it includes subtidal and peritidal carbonates (Angolo Limestone, 250–300 m thick), basinal marly limestones (Prezzo Limestone, 10–15 m), carbonate platform facies (Esino Limestone, 600–700 m) characterized at the top by a regressive carbonate unit (Calcare Rosso), testifying to subaerial exposure. The Calcare Rosso is covered by peritidal (Breno Fm.) and later subtidal limestones (Calcare Metallifero Bergamasco, 80–100 m), followed by 150–300 m of lagoon marls and limestones (Gorno Fm.), laterally interfingering with deltaic sandstones (Val Sabbia Sandstone). The youngest unit in the thrust stack is represented by terrigenous-carbonate sabkha facies deposits of the San Giovanni Bianco Fm. (about 100 m preserved), including gypsum layers (Fig. 5).

This antiformal stack is bounded to the south by the Clusone fault which represents the detachment horizon developed along the San Giovanni Bianco Fm. The overlying Upper Triassic succession mainly consists of the carbonate platform system of the Dolomia Principale and coeval basinal facies (more than 1 km thick), exposed immediately south of the Clusone fault.

The Grem–Val Vedra Transverse Zone (GVTZ) is confined within the Middle Triassic to Carnian units, between the Valtorta–Valcanale and the Clusone faults. In the following sections, we first describe the different tectonic units within the antiformal stack and then the major structures within the GVTZ, before presenting some results from the 3D structural modelling.

3.1 The tectonic units

The tectonic units were defined through original 1:5,000 to 1:10,000 field mapping improving the available 1:10,000 geological sheet "Roncobello" (Regione Lombardia, 2000) and the 1:50,000 Geological map of the Bergamo Province (Forcella and Jadoul 2000). Tectonic units are numbered

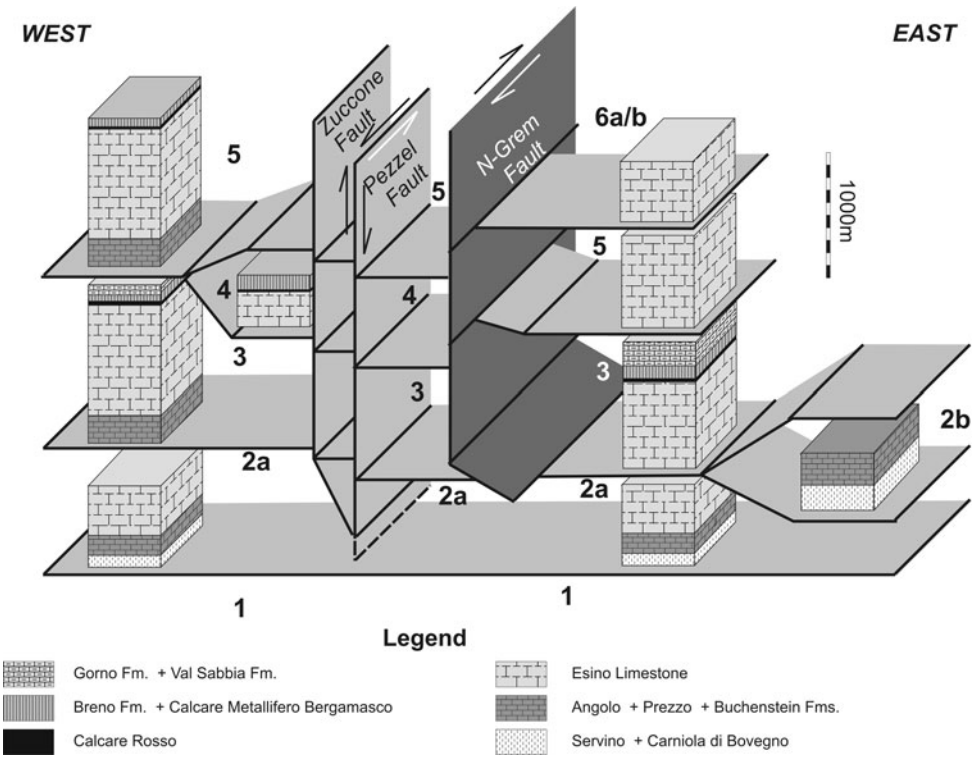

Fig. 5 Schematic reconstruction of the stratigraphic and structural setting of the study area

according to their structural position, from bottom to top (Figs. 3, 4, 5). The results of stratigraphic and structural analyses, performed along the whole of the GTVZ in the different tectonic units, are summarized in the following paragraphs.

3.1.1 Unit 1 (Trabuchello–Cabianca Anticline)

Unit 1 belongs to the Orobic Anticline belt forming the structurally lowermost unit of the area. The Early Permian to Olenekian succession is folded into an open anticline with sharp and regular flanks and angular hinges, interpreted as a fault-bend fold related to the propagation of a deep south-verging thrust surface (Schönborn 1992b). A N–S trending fault crosses this unit to the north of the study area, tipping out around Baite di Mezzeno (Forcella and Jadoul 2000), north of the Valtorta–Valcanale fault. No relationships occur between this structure and the GVTZ, as they belong to different tectonic units.

The anticline wedges out under the imbricate Triassic units along the Valtorta–Valcanale fault (Fig. 4).

3.1.2 Unit 2 (Valcanale unit)

Unit 2 develops south of the Valtorta–Valcanale fault, and consists of an Olenekian to Ladinian succession including thin layers of the Prezzo and Buchenstein Fms. at the base of the Esino Limestone. In the upper Val Secca (east of Roncobello), the unit is folded in an open asymmetric anticline with a N-dipping axial plane that clearly supports a southward transport during thrust stacking. The thickness of the unit increases eastward and is well exposed all along Val Canale. A minor duplex structure due to the tectonic repetition of the lower Angolo Fm. (2b in Fig. 3) is present below the basal thrust surface of unit 3. The whole unit has been tilted southward due to the successive propagation of the Trabuchello–Cabianca Anticline (unit 1; sections B–B' and C–C' on Fig. 4). Field data suggest that unit 2 disappears southward at depth below the overlying unit 3. The N–S Zuccone fault cross-cuts unit 2 to the north, forming a complex horse-tail branching termination exposed along Valsecca, east of Roncobello.

3.1.3 Unit 3 (Branchino unit)

Unit 3 forms the left side of Val Secca, the Corno Branchino massif, and a large part of Val Vedra. It is characterized by an Olenekian to Upper Carnian succession, strongly deformed along the GVTZ. The overturned syncline of Corno Branchino is one of the most peculiar elements of this unit. We interpret this fold as a footwall syncline related to the emplacement of higher thrust sheets now eroded in this area. The axial surface dips N–NE, indicating a top-to-S transport direction during the growth of the thrust stack. Increasing distortion of the axial surface from E–W to N–S at the northern tip of the N-Grem fault,

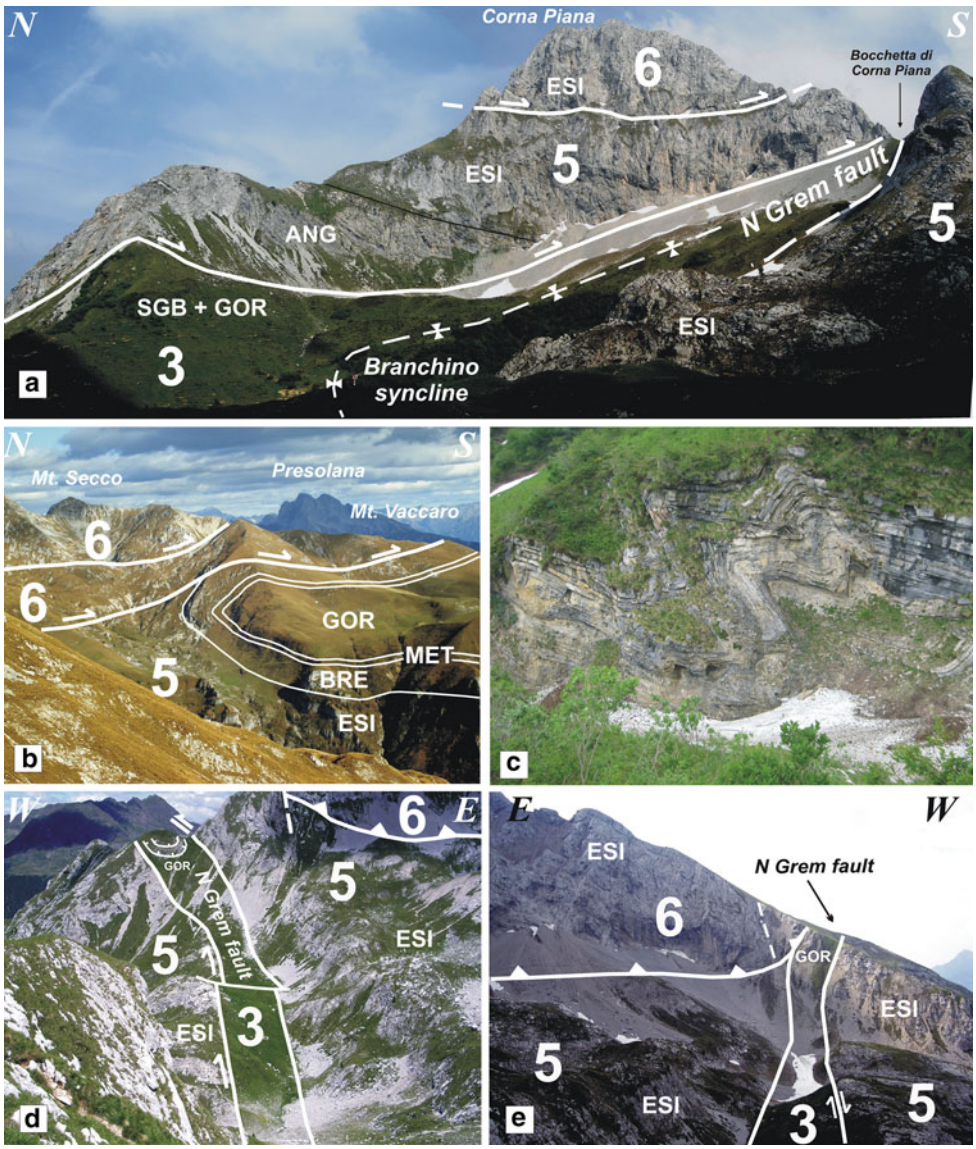

Fig. 6 Field photos of the main structures in the study area; their location is shown in Fig. 3. **a** The uppermost thrust sheets: the Menna-Nossana (*5*), and the Arera (*6*) units exposed on the western slopes of Corna Piana; **b** the Mt. Vaccaro syncline below Mt. Vaccaro, view from Mt. Golla to the east; **c** asymmetric parasitic folds along the lower limb of the Mt. Vaccaro syncline in the upper reaches of the Parina valley; **d** the southern termination of the Corno Branchino syncline E of Mt. Arera at the Bocchetta di Corna Piana, view to the north from the western slopes of Mt. Arera. Compare with **a**. **e** Relationships between the N-Grem fault and the floor thrust of the Mt. Arera unit along the western slopes of Mt. Area, just south of **d**

west of Corna Piana (Figs. 2, 3) suggests that the right-lateral slip along the fault was coeval to the growth of the fold during thrust emplacement. A syncline with an overturned limb and similar characters crops out along the right side of Val Vedra, south of Mt. Vetro. Despite its smaller amplitude and wavelength, this fold is very similar to the Branchino syncline. Both structures are suggested to have formed in the footwall as drag folds during southward thrust motion.

Northwest of Oneta three small tectonic windows expose unit 3 below unit 5 along the Riso Valley. The top of the underlying unit is marked by calc-mylonites formed between the marly limestones of the Gorno Fm. (unit 5) and the characteristic layers of tectonic "carniola" belonging to the underlying San Giovanni Bianco Fm. (unit 3). Further constraints on the deep setting of unit 3 come from subsurface geological observations made during the construction of the Riso-Parina mining tunnel (Rodeghiero and Vailati 1978; trace of the tunnel in Figs. 2, 3). As shown by the E–W trending geological cross-sections along the southern sector of the Grem fault (Fig. 8), which integrate our own surface observations with subsurface data from Rodeghiero and Vailati (1978), the eastern portion of unit 3 is lowered by a lateral ramp, progressively passing eastward to the floor thrust of the unit. The N–S trending ramp directly juxtaposes the Esino Limestone of the overlying unit 5 to the deformed Gorno Fm of unit 3. This structural setting conditioned the excavation of the Riso-Parina tunnel, which runs parallel to the ramp for more than 2 km, before turning westward into the San Giovanni Fm. of unit 3 (Rodeghiero, personal communication). Mylonitic layers formed in the Gorno Fm., similar

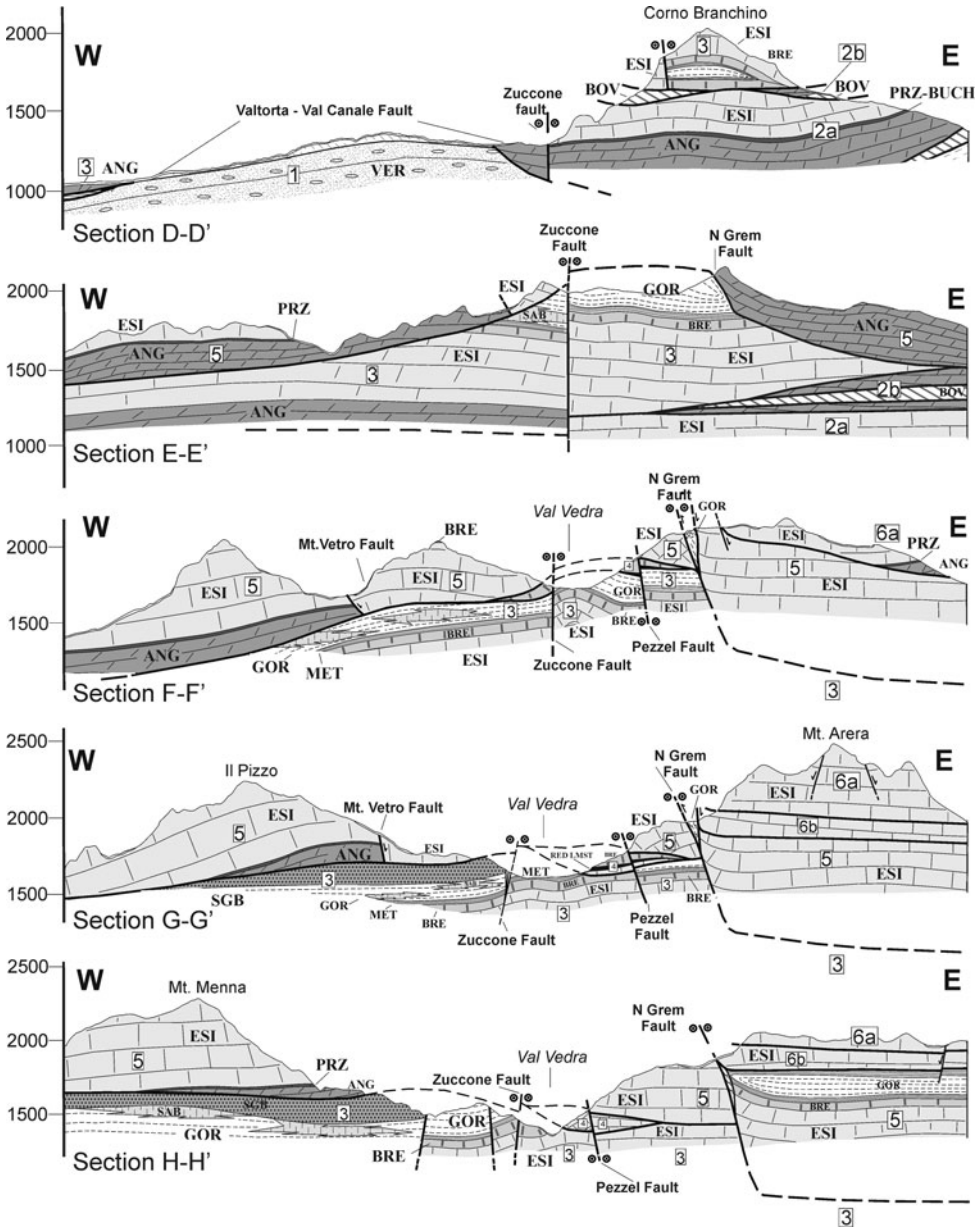

Fig. 7 E–W cross sections across the GVTZ (N-Grem fault) N of the Mt. Vaccaro syncline. Traces of cross sections are reported on the geological map of Fig. 2

to the ones exposed along the Riso valley, characterize this fault surface along the N–S track of the Riso-Parina tunnel. This lateral ramp represents the deep expression of the southern portion of the Grem fault. According to our data, unit 3 continues at depth also in the southern portion of the study area.

3.1.4 Unit 4 (Val Vedra unit)

Unit 4 is a small horse formed between units 3 and 5 (Figs. 3, 4, 5), exposed along Val Vedra. This previously unknown unit has a maximum thickness of 100 m and consists of a succession spanning from the upper part of the Esino Limestone to the lower part of the Breno Fm.

3.1.5 Unit 5 (Menna-Nossana unit)

Unit 5 is the largest thrust sheet occurring in the study area (Figs. 3, 4, 5, 6, 7, 8). It consists of a thick and continuous Anisian to Carnian carbonate succession largely including the Angolo and Esino Limestone which forms the Mt. Menna, Corna Piana and Mt. Arera massifs. The unit is split into three sectors by the Zuccone and Grem faults of the GVTZ (Fig. 3). Previous authors considered them as different units, but no significant lithological, stratigraphic and structural differences occur among these sectors. In addition, the stratigraphic continuity of the Carnian succession across the central and eastern sectors south of Oneta, where the southern segment of the Grem fault tips out, shows that they all belong to the same thrust sheet.

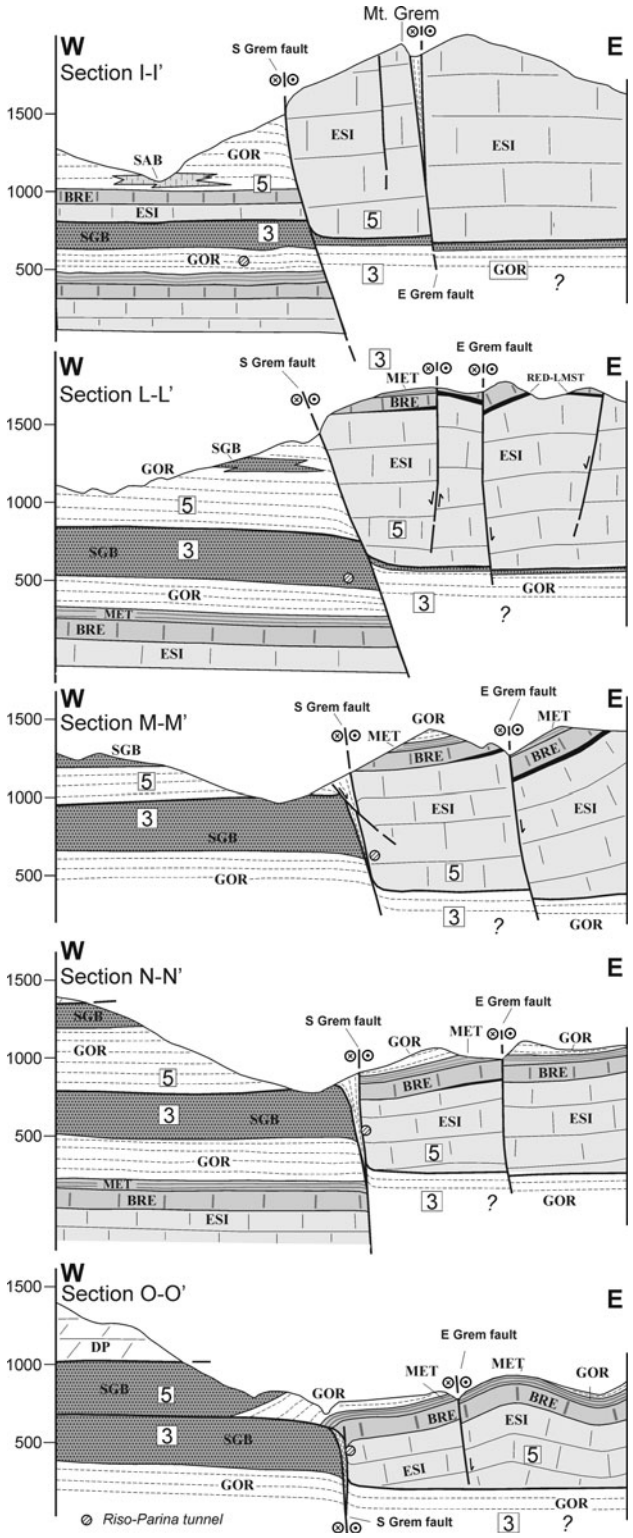

Fig. 8 E–W cross section across the GVTZ (S-Grem fault segment) to the south of the Mt. Vaccaro syncline

The westernmost sector is characterized by a south-verging sole thrust flooring the rigid body of the Mt. Menna–Mt. Vetro massif. The same unit is gently folded south of the summit of Mt. Menna towards the village of Zorzone, along the western side of Val Vedra. The floor thrust of the unit is cut by the Zuccone fault (Figs. 2, 3). Normal faults are exposed in the NE portion of the unit around Mt. Vetro. As this fault system ends west of the Zuccone fault and does not cross-cut the thrust surface at the base of unit 5 (Figs. 2, 3), it may be interpreted as a pre-thrusting structure, passively transported during thrust stacking. A more complex geometrical setting can be recognized to the east, where unit 5 is cut by the Grem fault, which separates the central and the eastern sectors, and by other minor faults forming minor blocks and tectonic repetitions. The central sector (Zambla, Val Parina; Fig. 3) between the Grem and Pezzel faults behaved as a rigid wedge-shaped block partially juxtaposed on unit 3 in its northern part and in contact with the eastern portion of unit 5 south of Alpe Arera (Fig. 3). This sector of unit 5 thins out to the south, due to a ramp cutting through the folded Ladinian carbonates and reaching the Carnian succession (Fig. 5) as documented by small tectonic windows along the Riso valley, in which the San Giovanni Bianco Fm. of the underlying unit 3 is exposed below mylonitic limestones of the Gorno Fm. of unit 5. South of Oneta, where the southern segment of the Grem fault tips out within the Gorno Fm., the central and eastern sectors of unit 5 directly merge, confirming that the three sectors belong to the same tectonic unit. The eastern sector of the unit also shows a lateral ramp with unit 3 around Passo Branchino (Fig. 6a) passing to the transpressional Grem fault southward, where unit 3 is partially covered by the uppermost thrust sheets of the stack (unit 6).

The E–W trending Vaccaro syncline, which formed during the southward thrusting of the higher thrust sheets (units 5 and 6; Fig. 4, section C–C', and Fig. 6b), occurs south of Mt Arera. The fold has a N-dipping axial surface and is characterized by parasitic folds on its normal flank (Fig. 6c and site S4 in Fig. 3). To the west the whole structure, extending from Mt. Vaccaro to Mt. Arera, is sharply cut by the Grem fault system without any distortion of the axial surface. Forcella and Jadoul (2000) suggested that the Vaccaro and Branchino synclines were part of the same structure, then displaced by the Grem fault with a right-lateral throw of at least 1.5–2 km. However, new field data indicate that the Vaccaro syncline belongs to a higher structural level (unit 5) with respect to the Branchino syncline (unit 3), implying that they cannot be used as markers to evaluate the displacement along the Grem fault.

North of Mt. Grem, along Val Parina, the Esino Limestone is partially back-thrust onto the Carnian units at the core of the Vaccaro syncline. The E–W back-thrust is bounded to the west by the southern segment of the Grem fault (S Grem fault on Fig. 2) and by a NNW–SSE trending right lateral strike-slip structure to the east, here named the

Eastern Grem fault (E Grem fault on Fig. 2), which cuts across the unit near the top of Mt. Grem (Fig. 3, site S8).

According to subsurface observations (Rodeghiero and Vailati 1978) along the Riso-Parina tunnel (550 m a.s.l.), the floor thrust of the eastern sector of unit 5 gently dips southward running within the Esino Limestone, so that the sole thrust of unit 5 is much deeper than to the west of the Grem fault.

3.1.6 Unit 6 (Arera unit)

Unit 6 forms the klippe of the Corna Piana–Mt. Arera massif which is exposed east of the Grem fault (Figs. 3, 4). This unit also includes an Anisian to Ladinian succession with the Angolo, Prezzo and Esino Limestone (Fig. 5). The basal thrust is well exposed along the northern slope of Corna Piana, where it forms a ramp dipping between 30° and 40° to the north (Fig. 4), marked by calc-mylonites up to 3 m thick. Southward, along the southern slope of Mt. Arera, the thrust surface is nearly flat, and parallel to the bedding of the less competent Carnian units documenting a ramp-and-flat geometry. Duplex structures, revealed by the occurrence of small horses consisting of cataclastic layers in the Esino Limestone, occur along the southern part of the floor thrust of the unit (6b in Fig. 3). In addition, small normal faults displace the thrust sheet north of Corna Piana (Fig. 2). Unit 6 is the uppermost unit of the stack and its structural position is comparable with the Presolana unit east of Val Seriana (Forcella 1988; Zanchi et al. 1990b). The occurrence of calc-mylonites along their floor thrusts in both units suggests similar deformation mechanisms during thrusting.

3.2 The main faults of the GVTZ

The main faults of the GVTZ are represented by the Grem, Zuccone and Pezzel faults (Figs. 2, 3). The most important structure is the Grem fault which has a NNW–SSE trend and occurs just south of Passo Branchino passing along the western flank of Corna Piana and along the SW flank of Mt. Arera. The fault extends southward along the western slope of Mt. Grem, tipping out NW of Oneta (Figs. 2, 3). A selection of E–W cross-sections across the Grem fault is shown in Figs. 7 and 8. The fault has always been considered as a unique continuous structure. However, field data suggest that it consists of two different segments with different characteristics and structures.

3.2.1 Grem fault, northern segment

The northern segment of the Grem fault (labelled N Grem fault on Figs. 2, 3, 4, 5, 6, 7) is marked by a few meters thick tectonic slice consisting of strongly deformed and folded marly limestones attributed to the Gorno Fm. of unit 3 (Figs. 6d, e; 7, cross sections F–F', G–G', H–H'). In this area, the northern segment represents the steep lateral ramp for units 5 and 6, as suggested by the geometry of their thrust surfaces west of Mt. Arera (Fig. 7, cross sections F–F', G–G', H–H').

The termination of this fault segment north of Passo Branchino, as well as the lateral closure of unit 3 east of Corno Branchino, suggests that the fault is confined within units 3, 5, and 6. Dextral motion with a slight oblique reverse component is supported by striations, growth fibers, and pressure solution cleavage along the fault plane (Fig. 3, sites S5, S7, S9a). These data are consistent with dragging and torsion of the Corno Branchino syncline, which turns progressively clockwise from an E–W to a N–S trend along the fault trace (Fig. 3, S1, S2 and S3). This suggests that the northern segment of the Grem fault was already active during the growth of the Branchino syncline.

3.2.2 Grem fault, southern segment

The southern segment of the Grem fault (labelled S Grem fault on Figs. 2, 3, 4, 5, 6, 8) separates the central and eastern sector of unit 5. It shows different features with respect to the northern segment, as it becomes steeper and continues southward as a tear fault parallel to the thrust propagation direction (Fig. 8). The southern segment of the fault also shows a significant apparent vertical displacement among corresponding stratigraphic levels reaching a maximum throw of a few hundred meters along the reconstructed cross-sections (Fig. 8), which results from dextral oblique motion along the exposed portion of the fault system (Fig. 3). A similar amount of the maximum horizontal displacement can be also evaluated. As shown in Fig. 3 and in cross sections of Fig. 8, moving southward from Val Parina, the throw along the southern segment decreases and the fault ends SW of Oneta where it tips out in a N–S trending flexure. South of Mt. Arera, part of the displacement occurring along the fault within unit 5 is transferred to the Eastern Grem fault (labelled E Grem fault on Figs. 2, 3, 8), which shows a similar style, and by the successive back-thrusting of the Esino Limestone upon the Vaccaro syncline.

The southern segment of the Grem fault nucleates on a deeper wrench fault represented by the lateral ramp of the sole thrust of unit 5. The lateral ramp is responsible for the lateral juxtaposition at depth of the San Giovanni Fm. of unit 3 with the Esino Limestone of unit 5, as observed along the N–S segment of the Riso-Parina tunnel (Figs. 2, 3). Units 3 and 5 are here separated by a N–S trending, steep cataclastic to mylonitic shear zone at least 10–20 m thick, enclosing strongly deformed layers of the Gorno Fm. The lateral ramp can be observed also at a depth of about

200 m south of Oneta, where the southern fault segment tips out at the surface. The ramp has been successively cross-cut by a vertical strike-slip fault which corresponds to the presently exposed segment of the fault. This shallower portion of the fault accommodates the vertical offset between the eastern and central sectors of unit 5. The total vertical displacement progressively increases from the southern tip of the fault (Oneta) toward the north (Val Parina), where the eastern block is uplifted several hundred meters with respect to the central sector of the unit due to back-thrusting on the Vaccaro syncline (Fig. 8).

3.2.3 Eastern Grem fault

This fault is an important component of the southern portion of the GVTZ, running directly east of Mt. Grem. North of Mt. Grem the fault includes a strongly deformed tectonic slice of marly limestones belonging to the Gorno Fm. and displaces the Val Parina back-thrust with a small dextral off-set. We suggest that the East Grem fault can be interpreted as a minor tear fault accommodating a differential displacement along the back-thrust. Zn-related ore deposits occur just east and south of Mt. Grem along the fault.

Mesoscopic observations (S8 in Fig. 3) and field mapping (Fig. 2) suggest a right-lateral displacement of about one hundred metres associated to a comparable vertical throw (Fig. 8), which progressively decreases southward. The fault tips out SE of Oneta, similarly to the southern segment of the Grem fault.

3.2.4 Zuccone fault

The Zuccone fault is a composite N–S to NNE–SSW oriented left-lateral system crossing the western flank of Val Vedra. It dips steeply westward and extends for about 5–6 km ending with a horse-tail branching termination into the lowermost unit just south of the Valtorta–Valcanale fault (Figs. 2, 3). To the south, the fault dies out within the plastic Carnian beds; its displacement is partially accommodated by the syncline developed west of the fault. The displacement of the overturned syncline exposed south of Mt. Vetro (unit 3), as well as kinematic indicators along the main fault planes, support left-lateral motion along the fault. The Zuccone fault was probably active during the emplacement of units 5 and 4, similar to the northern segment of the Grem fault and thus behaved as a syn-thrust tear fault. At least 250 m of vertical offset was accommodated by this fault (Fig. 7). The hanging wall (unit 5, Mt. Menna) is clearly downthrown westward and this may be partially related to a later reactivation of the structure as a normal fault. This would account for the apparent dextral displacement of the thrust surfaces along the northern part of the fault.

3.2.5 Pezzel fault

The NE-SW trending and E-dipping Pezzel fault bounds to the west the central sector of unit 5 (Figs. 2, 3; 7, cross-sections F–F', G–G', H–H'). Vertical mylonitic foliations oblique to the fault strike suggest a left-lateral motion, as also indicated by previous authors (Rodeghiero and Vailati 1978). A minor extensional reactivation affected the southernmost part of the fault. The southern continuation of the fault bounds the eastern side of the Val Vedra half-window, juxtaposing unit 5 and unit 3.

4 3D structural modelling

The 2D representation of geological structures shown in traditional geological maps is often inadequate to represent exhaustively the structural intricacy of a complex area. The use of 3D software techniques for structural modelling gives the opportunity to analyse, reconstruct and visualize more efficiently complex structures. A 3D model can also be useful to validate structural interpretations based on 2D field data and to eventually check different hypotheses when surface structural data are poor or uncertain. Several examples of integration of different type of data to reconstruct subsurface geological objects have been published, with particular regards to those based on field data (de Kemp 1999, 2000; Husson and Mugnier 2003; Maxelon and Mancktelow 2005; de Kemp et al. 2006; Zanchi et al. 2009). On the basis of these previous experiences, 3D models of the Branchino and Vaccaro synclines have been elaborated (Figs. 9, 10, respectively) and will be discussed below.

In the study case, the representation of the geometrical features of folds formed in different structural situations helps to better understand the complex kinematics of the study area. The Branchino syncline has been chosen in order to describe the complex geometry of folds formed along a transpressional fault, which cannot be reliably represented though conventional 2D cross sections, and is then compared to the simpler Vaccaro syncline due to south-verging thrusting.

Three main typologies of geometric features and related attributes were managed in a GIS-database and later exported into the 3D modelling software Move (© Midland Valley Exploration Ltd.): (1) a digital elevation model (DEM) of the topographic surface (obtained using the 20 m pixel size Digital Terrain Model of Regione Lombardia), (2) stratigraphic and tectonic boundaries, traces of fold axial surfaces as two dimension lines, (3) structural data as point features identified by x, y coordinates.

After having imported all objects in Move, linear features have been projected vertically onto the DEM in order

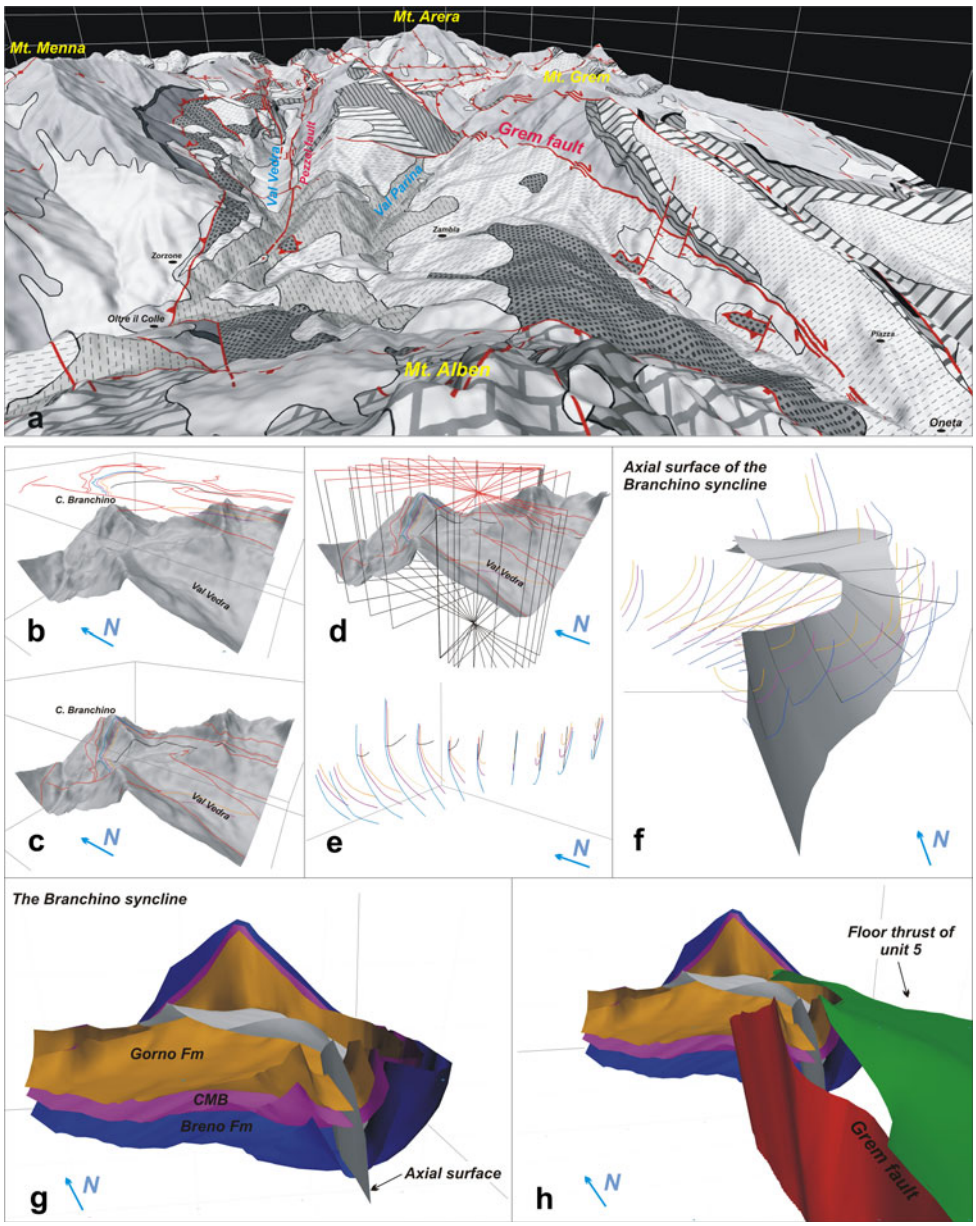

Fig. 9 3D model of the GVTZ. **a** Geological structural map draped on the 20 m pixel size DEM of Regione Lombardia. **b–f** The workflow used to integrate field data as lithological boundaries, fault and thrust surface traces in a 3D environment to build a 3D cross sections grid. **g**, **h** Reconstructed 3D surfaces of the Corno Branchino syncline, the N-Grem fault and the floor thrust of the Menna-Nossana thrust sheet (unit 5)

to obtain a 3D geological map (Fig. 9a) showing the main stratigraphic and structural elements in the northern part of the GVTZ. Geometrical constraints (Chilès et al. 2004) to be used for the construction of a grid of cross sections have been defined based on field structural analyses and also on orientation analyses of the collected data through Move. The analysis has mainly concerned the attitude of planar and linear features such as bedding, faults, foliations, fold axes and axial planes (Figs. 9, 10). Particular care has been given to the attitude of mesoscopic features (bedding and cleavage), in order to provide an accurate description of this complex structure, and to better evaluate its geometry.

A grid with about 20 geological cross sections has been drawn in Move; the strike and the extent of each section have been chosen in order to introduce all the constraints derived from field structural analyses into our model. The surfaces representing thrust planes, strike-slip faults, stratigraphic boundaries and axial surfaces of folds have been then obtained interpolating the corresponding linear features contained in the cross sections grid. The obtained models have been refined until a fit with the field data was satisfactory.

4.1 Branchino syncline

The Branchino and Vaccaro syncline folds have been built using cross sections perpendicular to the strike of axial planes (Fig. 9f, g), whereas both parallel and perpendicular

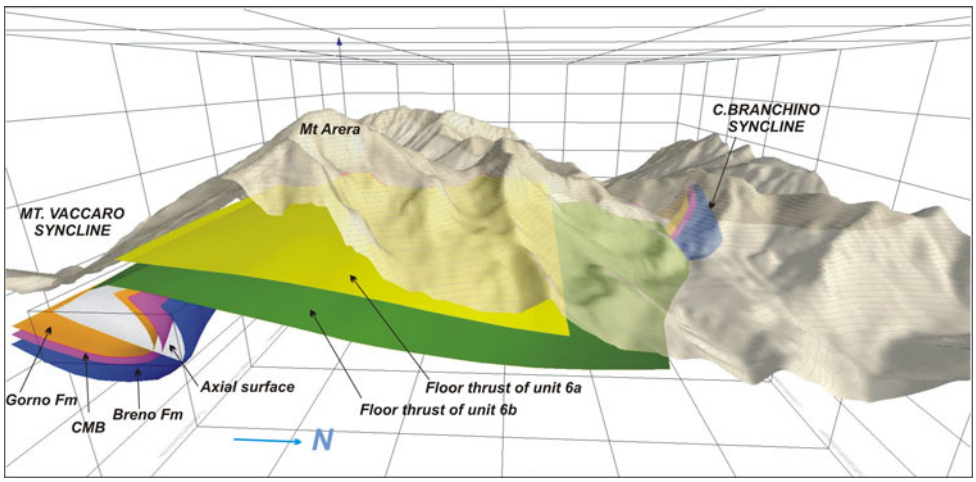

Fig. 10 3D visualization of the Mt. Vaccaro syncline, developed beneath the floor thrust of the Arera unit (6b in Fig. 3)

cross sections were used to reconstruct fault surfaces (Fig. 9h). The 3D model of the Branchino syncline helps to constrain the extension of this structural object at depth and to clearly visualize its geometrical relationships with the boundary faults of the transverse zone (especially the northern segment of the Grem fault) and the main thrust surfaces. It illustrates a significant example of a syn-thrusting transpressional deformation.

The constructed cross sections grid allowed to define in detail the complex folding pattern of the Branchino syncline. Three main stratigraphic boundaries (Esino Lmst.–Breno Fm., blue; Breno Fm.–CMB, purple; CMB–Gorno Fm., orange) have been modelled as 3D surfaces, together with the axial plane surface of the syncline (grey). Just southeast of Corno Branchino the syncline broadly trends E–W, with a horizontal axial plane. Moving southwards the dextral transpression active along the N-Grem fault causes the folds to deflect clockwise, with a progressive steepening of the axial plane surface (Fig. 9g).

4.2 Vaccaro syncline

The Vaccaro syncline has been modelled using the folded stratigraphic boundaries exposed on the E side of the Grem fault. As shown in Figs. 2 and 10, the axial plane surface of the Vaccaro syncline displays a minor northwards deflection near the contact with the N-Grem fault. In fact, this structure preserves its original geometrical features, which formed before right-lateral motion along the Grem fault.

5 Structural evolution of the GVTZ

Two main compressive stages affected the central Southern Alps before the intrusion of the Upper Eocene–Lower Oligocene Adamello batholith (Brack 1981; Laubscher 1985; Doglioni and Bosellini 1987; Schönborn 1992a; Castellarin et al. 2006; Zanchetta et al. 2011; D'Adda et al. 2011). The two deformational events include the activation of thrust and strike-slip faults, suggesting a close relationship between the evolution of the transverse zone and the progressive growth of the thrust belt (Fig. 11).

5.1 First pre-Adamello compressional stage

According to Laubscher (1985) and Schönborn (1992a), the first Alpine compressive event resulted in the emplacement of the Orobic thrust sheet. Both basement and cover were thrust southward forming a thick imbricate thrust stack (Thrust system 1, Schönborn 1992a). This first compressive phase lasted for a rather long time and was Late Cretaceous in age, as pointed out by $^{40}Ar/^{39}Ar$ dating of fault-related pseudotachylytes along the Orobic thrust (Meier 2003; Zanchetta et al. 2011), and by the occurrence of the Cenomanian to Campanian turbiditic successions of the Lombardian Flysch (Doglioni and Bosellini 1987; Bernoulli and Winkler 1990; Zanchi et al. 1990a; Bersezio et al. 1993; Castellarin et al. 2006).

We attribute the emplacement of all imbricates south of the Valtorta–Valcanale fault (units 2–6 in Figs. 11a, 12a), which were stacked southward following a break-forward thrusting sequence, to this phase.

During the southward thrusting of the Arera unit (unit 6), the upper part of the Anisian to Carnian succession of the underlying Menna-Nossana unit (unit 5) was dragged along the thrust faults, which resulted in an E–W trending overturned footwall syncline (Vaccaro syncline, Fig. 11a). The N-Grem fault acted as the lateral ramp at the eastern termination of unit 6, with a dextral strike-slip component.

The continuation of the compression (Figs. 11b, 12b) caused the in-sequence stacking of the Menna-Nossana unit (unit 5) to the south, forming in its footwall the small horse

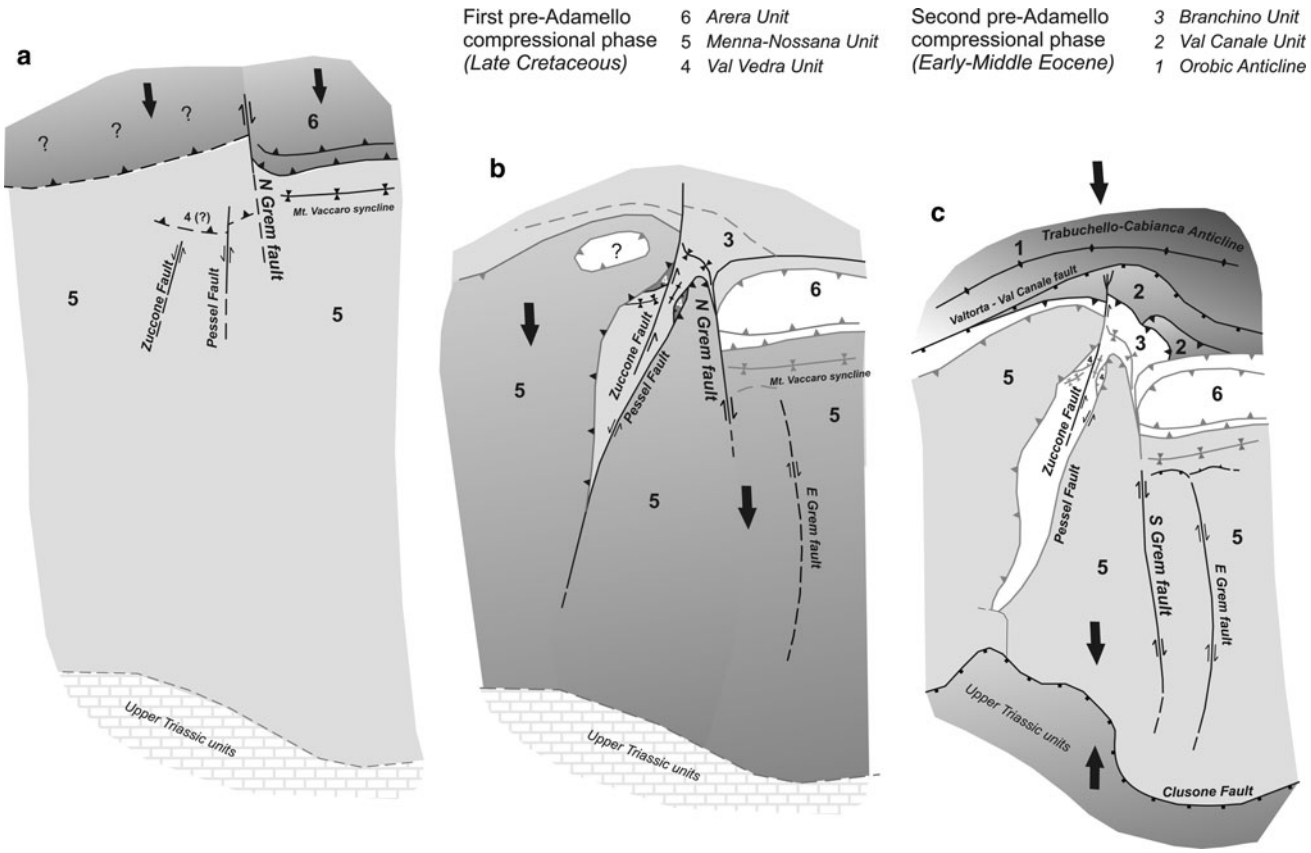

Fig. 11 Reconstructed tectonic evolution of the GVTZ. *Shaded dark grey units* with folds and structures showing *black symbols* are active during each deformational stage. **a** Nucleation of the Grem fault on an inherited paleotectonic lineament related to the Mesozoic evolution of the Lombardian basin. **b** The growth of the GVTZ. The Corno Branchino, originally developed as an E–W trending footwall syncline, is distorted along the GVTZ in a dextral transpression. The indenter of unit 5, bounded by the Zuccone and the N-Grem faults, formed during this deformation phase. **c** Reactivation of the southern termination of the Grem fault propagating southward. The back-thrust of unit 5 on the Mt. Vaccaro syncline is accommodated by dextral and vertical displacement along the S- and E-Grem faults

of the Val Vedra unit (unit 4). During this stage, the floor thrust of unit 6 was probably inactive and was passively transported southward on top of unit 5.

The northern segment of the Grem fault propagated downward at depth between units 3 and 5 (Figs. 11b, 12b), splitting unit 5 and causing a high-angle lateral ramp which lowered the southeastern portion of the floor thrust of unit 5, as suggested by the observations carried out along mine tunnels (Rodeghiero and Vailati 1978). Dextral strike-slip fault planes truncated the western termination of the Vaccaro syncline. The southward motion of unit 5 produced a drag fold in the Ladinian to Carnian succession of the underlying unit 3 (Branchino syncline), which was distorted and rotated clockwise along the northern segment of the Grem fault in a transpressional strain regime (Fig. 9). Vertically aligned tectonic slices made of strongly deformed and folded marly limestone of the Gorno Fm. along the northern sector of the fault (Fig. 6d, e and cross sections in Fig. 7) suggest the deep involvement of unit 3 during the growth of the northern segment of the Grem transpressional shear zone.

At the same time, the left-lateral Zuccone fault became active to the west, separating and displacing the western and the central sectors of unit 5 (Figs. 11b, 12b). A small overturned syncline with a N-dipping axial surface and a general E–NE trend formed in the Carnian succession of unit 3 south of Mt. Vetro and seems to be distorted by the Zuccone fault. The fold has the same structural position and similar geometrical characteristics as the Branchino syncline, suggesting that both folds were initially related to southward thrust propagation and were also possibly part of the same structure.

The southward thrusting of units 2a and 2b can be also related to this second stage of thrusting. We suggest that these units were stacked following the break-forward thrusting sequence of the upper units, which were then passively transported to the south. The presently south-dipping floor and roof thrusts are likely related to the passive tilting of the thrust surfaces during the formation of the Orobic Anticline, as suggested by south-verging asymmetric folds in unit 2. It is worth noting that the northern segment of the Grem fault

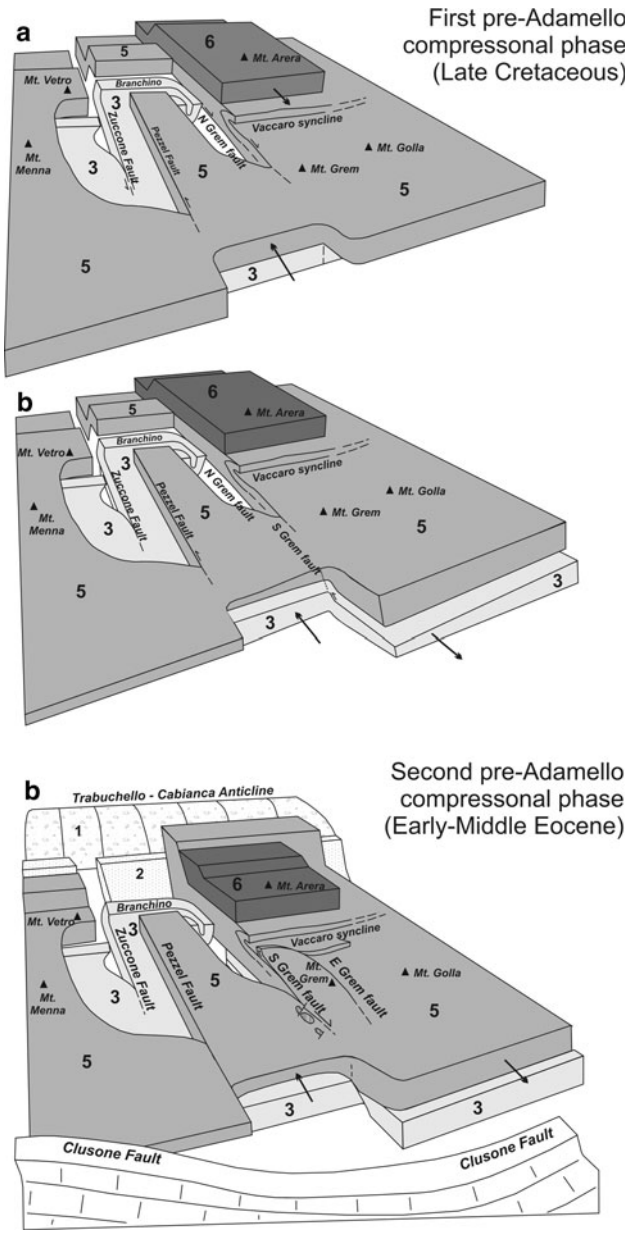

Fig. 12 *Block diagram* showing the evolution of the GVTZ; same steps as in Fig. 11

affects only units 3, 5 and 6, while units 2a and 2b extend continuously across the northern extension of this fault.

According to our reconstruction, this northern segment of the fault (and probably also the Zuccone fault) produced a ductile distortion of a thrust-related drag fold, which indicates coeval activity of thrusting and strike-slip faulting (Fig. 12a).

5.2 Second pre-Adamello compressional stage

A later compressive stage (Figs. 11c, 12c), with a different deformational style, involving deeper structural levels of the belt, occurred in the study area. This event has been related with the southward propagation of the Orobic Anticlines, wedging under the previous thrust sheets. Apparent N-verging back-thrusting and a general tilting of the Middle-Triassic carbonate units occurred during this second stage. Folding is especially evident along the forelimb of the Orobic Anticlines, where the Valtorta–Valcanale fault steeply dips southward (i.e. cross sections in Fig. 4). Further south, the Clusone fault was probably activated during the same stage (Figs. 11c, 12c), causing back-thrusting of the Upper Triassic strata onto the Middle Triassic ones (Zanchi et al. 1990b). This second compressive event is pre-Middle to Late Eocene, since the westernmost of the three anticlines (Cedegolo Anticline, Fig. 1b) is intruded by the south-western part of the Adamello batholith (Avio and Re di Castello units, Brack 1981, 1984), between 41 and 39 Ma (see Callegari and Brack 2002 for a summary). Furthermore, close to the study area, vertical E–W trending andesitic dikes dating between 42 and 39 Ma (U–Pb radiometric ages on zircons, D'Adda et al. 2011) cut across the stack of the Triassic strata.

The effects of the growth of the Orobic Anticlines-related thrust sheet is evident in the northernmost part of the Lower to Middle Triassic thrust pile, which has been steeply uplifted and tilted southward along the Valtorta–Valcanale fault along the forelimb of the Trabuchello–Cabianca Anticline. Regional tilting of thrust planes is also evident southward, as all the main thrust surfaces gently dip to the south all across the study area (Fig. 4). Folding of the whole thrust pile has been related by D'Adda et al. (2011) to back-thrusting of the Upper Triassic thrust sheets along of the Clusone fault, induced by the southward propagation of the deep thrust surfaces which underlay the Orobic Anticlines.

Important reactivations related to this second stage affect the southern segment of the Grem fault and the southeastern sector of unit 5. Out-of-sequence internal thrusts and back-thrusts of the eastern portion of unit 5 over the Vaccaro syncline just north of Mt. Grem can be related to a "buttress effect" given by the rigid mass of the Esino Limestones which forms this part of unit 5. The formation of these E–W trending thrust surfaces is related by clear geometrical relationships with the activation of the southern segment of the Grem fault and the Eastern Grem fault which partitioned dextral displacement along the transverse zone. A southward propagation of the fault system was accompanied by the uplift of Mt. Grem, which now forms a positive flower structure with respect to the western portion of unit 5e (Fig. 8).

We suggest that the described structures can be related to a general reactivation of previous discontinuities related to the important back-thrusting of the Upper Triassic units

along the Clusone fault, which was coeval, or possibly slightly younger than the formation of the Orobic Anticlines. No important reactivations are evident north of Alpe Arera, as most of the displacement was accommodated along the southern segment of the Grem fault and along the E–W structures of Val Parina. This also accounts for why the northern branch of the fault still preserves the structural setting achieved during the first deformational event.

6 Discussion

The first description of the Grem fault was given by De Sitter and De Sitter-Koomans (1949) who interpreted the structural setting of Val Vedra in terms of horst and graben structures. Schönborn (1992b, his Figs. 5, 6) suggested a continuation of the transverse zone up to the Trabuchello–Cabianca Anticline through the whole thrust pile of Triassic units, considering the fault system as a post-thrusting feature caused by the north directed indentation of a rigid wedge, bounded by NW–SE and NE–SW dextral- and left-lateral strike-slip faults. He also interpreted the GVTZ as a transtensional fault system, since most of the faults apparently show normal offsets, as previously suggested by De Sitter and De Sitter-Koomans (1949).

Our reconstruction supports a different tectonic scenario. All the analysed N–S strike-slip faults display reverse motions with dip-slip or oblique components. In addition, N–S trending folds formed within unit 3 along the northern segment of the Grem fault, as well as along Val Vedra, between the Zuccone and Pezzel faults, indicate that the GVTZ was active during transpressional deformations associated to intensive folding and high-angle reverse motions (Figs. 2, 3, 7, cross-sections F–F', G–G' and H–H'), rather than to a transtensional regime, as suggested by previous authors. The 3D reconstruction (Figs. 9, 10) helps to better understand the geometrical features and tectonic meaning of the different syn-deformational fold structures originated along the transpressional shear zone and thrust surfaces.

The Grem fault is the main structure of the GVTZ. It forms the lateral ramp of the higher units (unit 6 and eastern sector of unit 5) in the northern segment extending at depth across units 5 and 3 toward the south. Transpressional deformations associated with the rotation of the Branchino syncline along the fault zone are exposed north of Alpe Arera along the north segment of the fault zone. South of Mt. Arera, the deep ramp formed between units 3 and 5 exposed along the Riso-Parina tunnel is cross-cut by a vertical tear fault, now representing the southern continuation of the southern segment of the Grem fault at the surface. Local back-thrusting of the SE portion of unit 5 over the Vaccaro syncline, occurring between the main Grem fault and the Eastern Grem fault, results in the formation of the Mt. Grem positive flower structure.

According to our model, the Grem fault progressively propagated from north to south, moving from higher to lower structural levels during the oldest pre-Adamello compressional stages which affected the entire Southern Alps. We envisage a close kinematic relationship between the thrust sequence and the GVTZ. Our field data show that the northern segment of the Grem fault interacted with the Corno Branchino syncline and produced the distortion of its geometry in a transpressional regime. The across-strike deflection of syn-thrust ductile structures, resulting in the alignment of fold elements (axial planes, axes, fold limbs) parallel to the shear direction provide crucial information for understanding the kinematics of the transverse zone. First, it represents the evidence that movement in the Grem–Vedra Transverse Zone was coeval with thrust faults, since the ductile distortion of thrust-related folds can only be explained by a fault displacement active already during the initial stages of thrusting and folding. Secondly, since distorted thrust-related folds can be considered as drag folds, they represent good kinematic indicators to derive the overall shear sense within the transverse zone.

Second deformational stage is related to the emplacement of the Orobic Anticlines as fault-bend folds, following the model proposed by Laubscher (1985) and Schönborn (1992a, b), and is testified by a marked tilting of the thrust planes at the base of the imbricates made of Lower to Middle Triassic strata, which generally dip southward in the whole area. Back-thrusting along the Clusone fault, which also preceded the emplacement of the andesitic dikes showing the same age of the Adamello pluton (D'Adda et al. 2011), was probably responsible for the reactivation of the deep ramp along the southern segment of the Grem fault, between units 3 and 5 as a tear fault. Uplifting of the south-eastern sector of unit 5 was due to oblique motion along the fault and to local coeval and out-of-sequence thrusting just north of Mt. Grem between the southern segment of the Grem fault and the Eastern Grem fault.

Thomas (1990) provides a detailed description of possible controls on the location of transverse zones in thrust belts, such as the presence of deep pre-existing lineaments, pre-thrusting deformation of cover strata above deep faults or variations in mechanical stratigraphy. As the stratigraphy across the GVTZ does not change, and considering the Mesozoic stratigraphic successions of the Southern Alps, the best candidate for controlling the origin of the GVTZ can be identified in the presence of pre-existing lineaments. The Southern Alps have been affected by two major extensional events in the Norian (i.e. Jadoul et al. 1992) and Early Jurassic (i.e. Gaetani 1975; Winterer and Bosellini 1981; Bernoulli 2007), both responsible for the development of N–S striking normal faults which eventually led to the

opening of the Alpine Tethys during Middle Jurassic. In the central Southern Alps, these faults are highlighted by rapid thickness and facies changes in the Norian and Early Jurassic succession. The vertical throw of these faults was responsible for a displacement in the underlying older units as well. The presence of Norian and Early Jurassic faults in the younger units exposed to the south of the study area (Zanchi et al. 1990b; Schönborn 1992b; Bersezio et al. 1997) across lower Val Seriana suggests that the effect of these faults was probably recorded also at deeper stratigraphic and structural levels. Furthermore, evidence of a pre-compressional normal fault cutting the Ladinian–Carnian succession is observed in unit 5, where the extensional Mt. Vetro fault (Fig. 7, sections F–F' and G–G'), which was passively transported above the basal thrust of unit 5, can be explained as an extensional event pre-dating the Cretaceous compression. The possible reactivation of pre-compressional N–S striking normal faults during the N–S compression is supported by the occurrence of Jurassic normal faults marking the western border of the Sebino Trough along the same longitude as the GVTZ, although at higher structural levels in the thrust stack exposed just south of the Clusone fault (Bersezio et al. 1997; Zanchi et al. 1990b). Faults along Val Seriana have also been deduced from the facies distribution of Lower Jurassic deposits (Zanchi et al. 2009) and through reconstruction of back-stripping curves (Berra and Carminati 2010). The reactivation of these Jurassic faults south of the Clusone fault during the Alpine compressions is also documented by the development of a deep graben in the Norian to Jurassic units along the left side of the lower Val Seriana (Zanchi et al. 1990b).

Observations in the study area coupled with the stratigraphic and tectonic setting of the central Southern Alps strongly support the hypothesis that the development of the GVTZ during the first stage of thrust stacking was controlled by the presence of pre-Cretaceous faults that, considering the regional setting, were probably related to the Norian and/or Jurassic extension.

7 Conclusions

The Grem–Vedra Transverse Zone (GVTZ) is one of the N–S fault zones that interrupt the lateral continuity of the antiformal thrust stack developed within the Lower to Middle Triassic carbonate units of the central Orobic Alps. Our field data and analyses indicate that this important fault zone acted in a transpressional regime from the time when the oldest thrust sheets were emplaced. A pre-Adamello age for these compressive events is supported by a similar structural evolution recorded in the adjacent units of the belt (i.e. the Presolana antiformal stack; Zanchi et al. 1990a; D'Adda et al. 2011). The progressive southward and downward propagation of the northern segment of the Grem fault suggests close kinematic relationships with the thrust stack of the Middle Triassic units, which was emplaced following a break-forward thrust sequence. This indicates that the GVTZ nucleated and developed during the growth of the thrust pile. The transverse zone was then reactivated especially along the southern segment of the Grem and the Eastern Grem faults during a subsequent thrust event. This event was related to the emplacement of the out-of-sequence thrust system which caused the growth of the Orobic Anticlines in the northern sector of the belt.

The Grem fault is the main structural element of the transverse zone, which developed as a lateral ramp for units 3, 5 and 6. It is a composite dextral fault with two segments, the northern segment and the southern segment, which display different features, evolution and offsets. The northern segment of the Grem fault shows a maximum horizontal offset of about 1 kilometre, as suggested by the distortion of the Corno Branchino syncline within unit 3, whereas the observed offset along the southern segment does not exceed a few hundred meters, resulting in an apparent vertical displacement of more than 500 m. Dip-slip striations observed on the southern segment of the Grem fault can also suggest a reactivation of the structure as a normal fault. The presence of the wedge-shaped block in the central sector of unit 5 conditioned local strain partitioning with simultaneous distortion of the Branchino syncline and strike-slip motion along the northern segment of the Grem fault. A similar evolution is suggested for the Zuccone fault which was related to southward thrusting of the western sector of unit 5. As the Early to Middle Triassic stratigraphic successions exposed across the transverse zone are very similar in all the tectonic units, we suggest that the GVZT probably formed along inherited Norian to Jurassic N–S extensional faults.

Acknowledgments We are grateful to Franco Rodeghiero and Flavio Jadoul for fruitful discussions and field excursions in the study area. Franco Rodeghiero, who directly participated to the excavation of the Riso-Parina tunnel more than 30 years ago, gave an important contribution to the description of the structural setting along the main tunnels. The northern part of the study area was mapped by Paolo D'Adda during his master thesis. This work was supported with Italian F.A.R. grants from the University of Milano-Bicocca (2008–2009). The manuscript greatly benefited of the constructive reviews from A. Pfiffner and J.C. Blom. The editor of the journal, A.G. Milnes, is warmly thanked for encouragement and perfect editorial corrections of the final version. 3D modelling of has been performed with Move™ of the Midland Valley Exploration Ltd. We warmly thank its leader Alan Gibbs for including our Departments into the Academic Software License Initiative.

References

Bernoulli, D. (2007). The pre-Alpine geodynamic evolution of the Southern Alps: a short summary. *Bulletin fuer Angewandte Geologie, 12*(2), 3–10.

Bernoulli, D., & Winkler, W. (1990). Heavy mineral assemblages from Upper Cretaceous South- and Austroalpine flysch sequences (Northern Italy and Southern Switzerland): source terranes and paleo-tectonic implications. *Eclogae Geologicae Helvetiae, 83*, 287–310.

Berra, F., & Carminati, E. (2010). Subsidence history from a backstripping analysis of the Permo-Mesozoic succession of the Central Southern Alps (Northern Italy). *Basin Research, 22*, 952–975.

Bersezio, R., Fantoni, R., & Pessina, C. (2001). L'assetto strutturale del margine sudalpino-padano: contributo alla conoscenza del sottosuolo nel settore bergamasco. *Geologia Insubrica, 6*(1), 81–93.

Bersezio, R., Fornaciari, M., Gelati, R., Napolitano, A., & Valdisturlo, A. (1993). The significance of the Upper Cretaceous to Miocene clastic wedges in the deformation history of the Lombardian Southern Alps. *Géologie Alpine, 69*, 3–20.

Bersezio, R., Jadoul, F., & Chinaglia, N. (1997). Geological map of the Norian-Jurassic succession of the Southern Alps north of Bergamo. *Bollettino della Società Geologica Italiana, 116*, 363–378.

Blom, J. C., & Passchier, C. W. (1997). Structure along the Orobic thrust, Central Orobic Alps, Italy. *Geologische Rundschau, 86*, 627–636.

Brack, P. (1981). Structures in the southwestern border of the Adamello Intrusion (Alpi Bresciane, Italy). *Schweizerische Mineralogische und Petrographische Mitteilungen, 61*(1), 37–50.

Brack, P. (1984). Geologie der Intrusiva und Rahmengesteine des Südwest-Adamello (Nord-Italien). *Ph.D. Dissertation*, ETH no. 7612, Zurich, Switzerland.

Callegari, E., & Brack, P. (2002). Geological map of the tertiary Adamello batholith (northern Italy). Explanatory notes and legend. *Memorie di Scienze Geologiche, 54*, 19–49.

Carminati, E., & Siletto, G. B. (1997). The effects of brittle-plastic transitions in basement-involved foreland belts: the Central Southern Alps case (N Italy). *Tectonophysics, 280*, 107–123.

Carminati, E., Siletto, G. B., & Battaglia, D. (1997). Thrust kinematics and internal deformation in basement involved foreland fold and thrust belt: the Eastern Orobic Alps case (Central Southern Alps, Northern Italy). *Tectonics, 16*, 259–271.

Castellarin, A., Vai, G. B., & Cantelli, L. (2006). The Alpine evolution of the Southern Alps around the Giudicarie faults: A Late Cretaceous to Early Eocene transfer zone. *Tectonophysics, 414*, 203–223.

Chilès, J.P., Aug, C., Guillen, A., Lees, T. (2004). Modelling the geometry of geological units and its uncertainty in 3D from structural data: the potential-field method. In: *Proceedings Orebody Modelling and Strategic Mine Planning, Perth, WA*, 22–24 November 2004, pp. 313–320.

D'Adda, P., Zanchi, A., Bergomi, M., Berra, F., Malusà, M. G., Tunesi, A., et al. (2011). Polyphase thrusting and dyke emplacement in the central Southern Alps. *International Journal of Earth Sciences, 100*, 1095–1113.

de Kemp, E. A. (1999). Visualization of complex geological structures using 3-D Bezier construction tools. *Computer and Geosciences, 25*(5), 581–597.

de Kemp, E. A. (2000). 3D visualization of structural field data: examples from the Archean Caopatina Formation, Abitibi greenstones belt, Quebec, Canada. *Computer and Geosciences, 26*(5), 509–530.

de Kemp, E. A., Schetselaar, E. M., & Sprague, K. (2006). 3-D symbolization of L-S fabrics as an aid to the analysis of geological structures. *Computer and Geosciences, 32*(1), 52–63.

De Sitter, L. U., & De Sitter-Koomans, C. M. (1949). The geology of the Bergamasc Alps, Lombardia, Italy. *Leidse Geologische Mededelingen, 14B*, 1–257.

Doglioni, C., & Bosellini, A. (1987). Eoalpine and mesoalpine tectonics in the Southern Alps. *Geologische Rundschau, 76*, 735–754.

Fantoni, R., Bersezio, R., Forcella, F., Gorla, L., Mosconi, A., & Picotti, V. (1999). New dating of the Tertiary Magmatic products of the central Southern Alps, bearings on the interpretation of the Alpine tectonic history. *Memorie di Scienze Geologiche, 51*(1), 47–61.

Forcella, F. (1988). Assetto strutturale delle Orobie orientali, tra la Val Seriana e la Val Camonica. *Rendiconti della Società Geologica Italiana, 11*, 269–278.

Forcella, F., & Jadoul, F. (2000). *Carta Geologica della Provincia di Bergamo a scala 1:50.000 (Geological Map of the Bergamo Province, scale 1:50.000)*. Bergamo: Grafica Monti.

Gaetani, M. (1975). Jurassic stratigraphy of the Southern Alps: a review. In C. Squyres (Ed.), *Geology of Italy*, (pp. 377–402). Tripoli: The Earth Sciences. Society of the Lybian Arab Republic.

Gaetani, M., & Jadoul, F. (1979). The structure of the Bergamasc Alps. *Accademia Nazionale dei Lincei, (Rendiconti della Collezione di Scienze Matematiche Fisiche e Naturali), Serie VIII, 46*, 411–416.

Gaetani, M., & Jadoul, F. (1987). Controllo ancestrale sui principali lineamenti strutturali delle Prealpi lombarde centrali. *Rendiconti della Società Geologica Italiana, 10*, 21–24.

Gelati, R., Napolitano, A., & Valdisturlo, A. (1991). Results of studies on the Meso-Cenozoic succession in the Monte Olimpino 2 tunnel. The tectono-sedimentary significance of the Gonfolite Lombarda. *Rivista Italiana di Paleontologia e Stratigrafia, 97*(3–4), 565–598.

Husson, L., & Mugnier, J. L. (2003). Three-dimensional horizons reconstruction from outcrop structural data, restoration and strain field of the Baisahi anticline, Western Nepal. *Journal of Structural Geology, 25*(1), 79–90.

Jadoul, F., Berra, F., & Frisia, S. (1992). Stratigraphic and paleogeographic evolution of a carbonate platform in an extensional tectonic regime: the example of the Dolomia Principale in Lombardy (Italy). *RivistaItaliana di Paleontologia e Stratigrafia, 98*, 29–44.

Laubscher, H. P. (1985). Large scale, thin-skinned thrusting in the southern Alps: kinematic models. *Geological Society of America Bulletin, 96*, 710–718.

Maxelon, M., & Mancktelow, N. S. (2005). Three-dimensional geometry and tectonostratigraphy of the Pennine Zone, Central Alps, Switzerland and Northern Italy. *Earth-Science Reviews, 71*, 171–227.

Meier, A. (2003). The Periadriatic fault system in Valtellina (N-Italy) and the Evolution of the Southwestern Segment of the Eastern Alps. *Ph.D. Dissertation*, ETH no. 15008. Zrich, Switzerland.

Pieri, M., & Groppi, G. (1981). Subsurface geological structure of the Po plain, Italy. In: *Progetto Finalizzato Geodinamica Pubbl. 414*, Italy: CNR.

Rodeghiero, F., & Vailati, G. (1978). Nuove osservazioni sull'assetto geologico-strutturale del settore centrale del distretto piombo-zincifero di Gorno (Alpi Bergamasche). *L'Industria Mineraria, 29*, 298–302.

Schmid, S.M., Aebli, H.R., Heller, F., Zingg, A. (1989). The role of the Periadriatic Line in the tectonic evolution of the Alps. In M. P. Coward, D. Dietrich, R. G. Park (Eds.) *Alpine tectonics, vol 45* (pp. 153–171). Geological Society of London: Special Publications.

Schönborn, G. (1992a). Kinematics of a transverse zone in the Southern Alps, Italy. In McClay, K. (Ed.*) Thrust tectonics* (pp. 299–310), London: Chapman and Hall.

Schönborn, G. (1992b). Alpine tectonics and kinematic models of the central Southern Alps. *Memorie di Scienze Geologiche, 44*, 229–393.

Schumacher, M.E., Schönborn, G., Bernoulli, D., Laubscher, H.P. (1997). Rifting and collision in the Southern Alps. In A. Pfiffner, et al. (Eds.), *Result of NRP 20: Deep Structure of the Swiss Alps* (pp. 186–204). The National Research Program 20 (NRP/20). Basel: Birkhauser Verlag.

Thomas, W. A. (1990). Controls on locations of transverse zones in thrust belts. *Eclogae Geologicae Helvetiae, 83*(3), 727–744.

Winterer, E. L., & Bosellini, A. (1981). Subsidence and sedimentation on Jurassic passive continental margin. *American Association of Petroleum Geology Bulletin, 65*, 394–421.

Zanchetta, S., D'Adda, P., Zanchi, A., Barberini, V., & Villa, I. M. (2011). Cretaceous-Eocene compression in the central Southern Alps (N Italy) inferred from $^{40}Ar/^{39}Ar$ dating of pseudotachylytes along regional thrust faults. *Journal of Geodynamics, 51*, 245–263.

Zanchi, A., Chiesa, S., & Gillot, P. Y. (1990a). Tectonic evolution of the Southern Alps in the Orobic chain: structural and geochronological indications for pre-Tertiary compressive tectonics. *Memorie della Società Geologica Italiana, 45*, 77–82.

Zanchi, A., Chinaglia, N., Conti, M., De Toni, S., Ferliga, C., Tsegaye, A., et al. (1990b). Analisi strutturale lungo il fronte della Dolomia Principale in bassa Val Seriana (Bergamo). *Memorie della Società Geologica Italiana, 45*, 83–92.

Zanchi, A., Salvi, F., Zanchetta, S., Sterlacchini, S., & Guerra, G. (2009). 3D reconstruction of complex geological bodies: Examples from the Alps. *Computers and Geoscience, 3*, 49–69.